Electronic Supplementary Material (ESI) for Nanoscale Advances.

Rational design of carbon coated $Fe_2(MoO_4)_3$ nanosheet for lithium-ion storage with high initial Coulombic efficiency and long cycle life

Chennan Liang[a], Yuanxue Tao[a], Dekang Huang[a], Shu Li[a], Feifei Cao[a], Yanzhu Luo[a,], Hao Chen[a,]**

[a] College of Science, Huazhong Agricultural University, Wuhan 430070, PR China

Email: hchenhao@mail.hzau.edu.cn; luoyanzhu@mail.hzau.edu.cn

Supplementary Figures

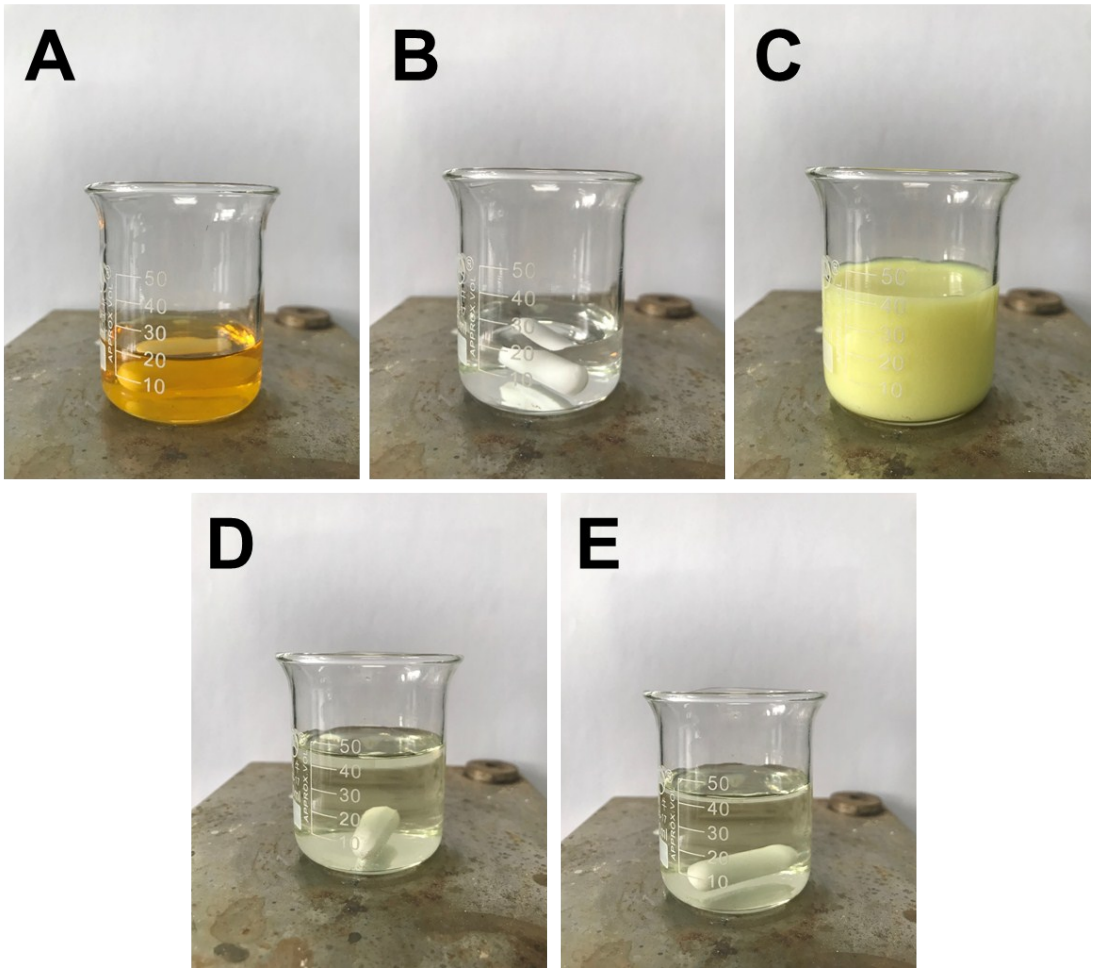

Fig. S1 Photograph of reaction solution at different stages: (A) $Fe(NO_3)_3 \cdot 9H_2O$ aqueous solution. (B) $(NH_4)_6Mo_7O_{24} \cdot 4H_2O$ aqueous solution. (C) Suspension obtained after the mixture of $(NH_4)_6Mo_7O_{24} \cdot 4H_2O$ and $Fe(NO_3)_3 \cdot 9H_2O$ solution. (D) Transparent

solution obtained after the addition of 2 mL HNO_3. (E) Transparent solution obtained after the addition of 1 g urea.

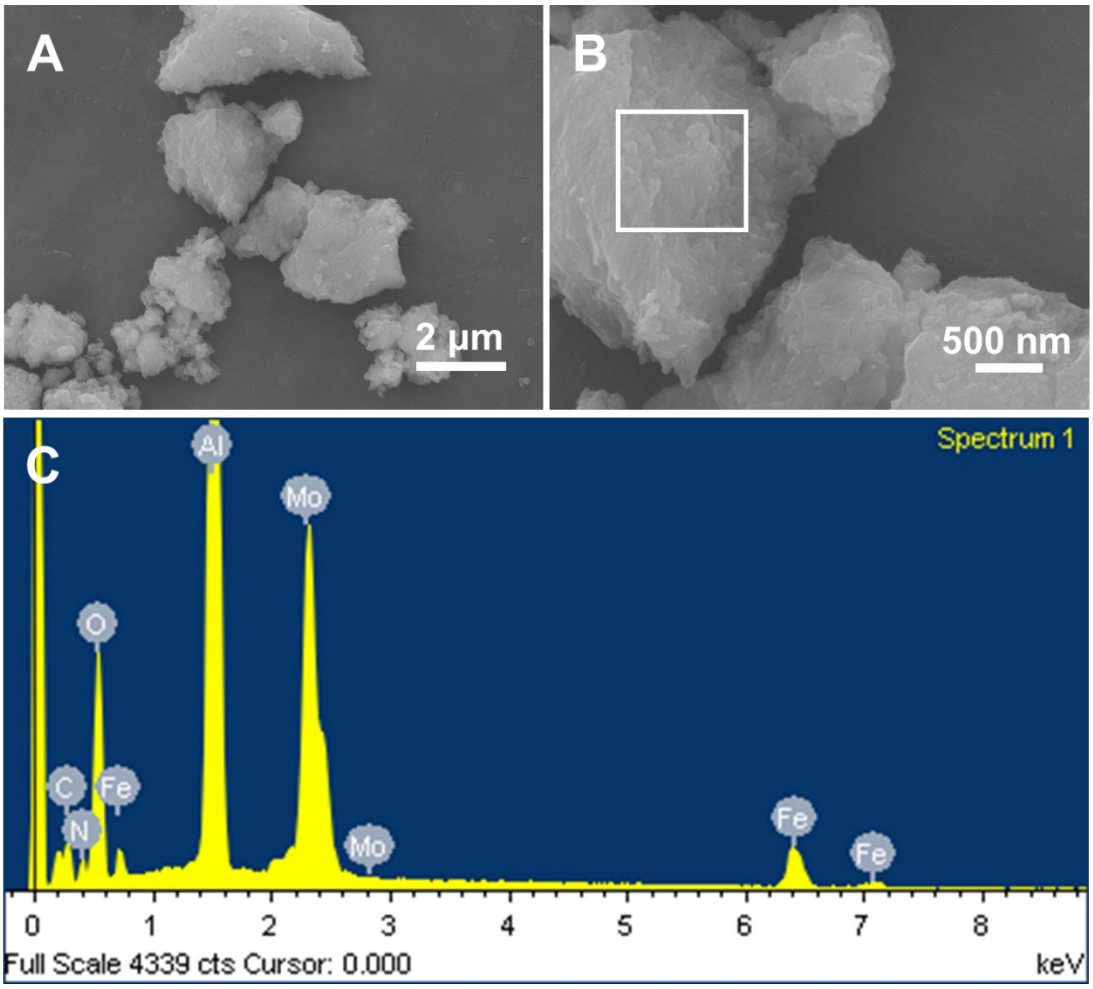

Fig. S2 SEM images (A, B) and corresponding EDS result (C) of intermediate yellow precipitations.

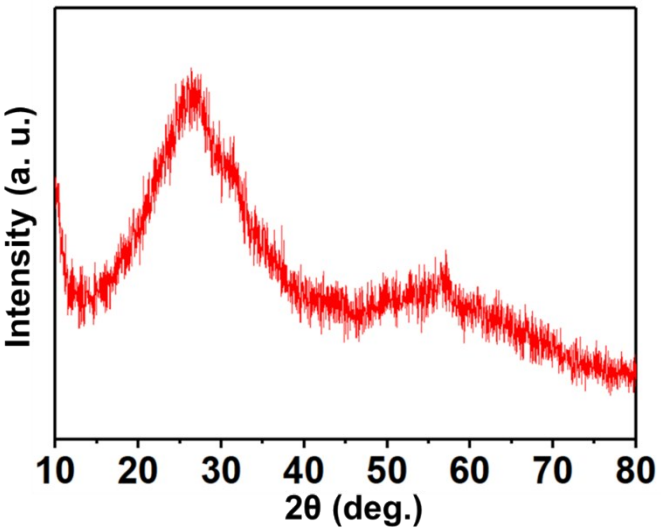

Fig. S3 XRD pattern of intermediate yellow precipitations.

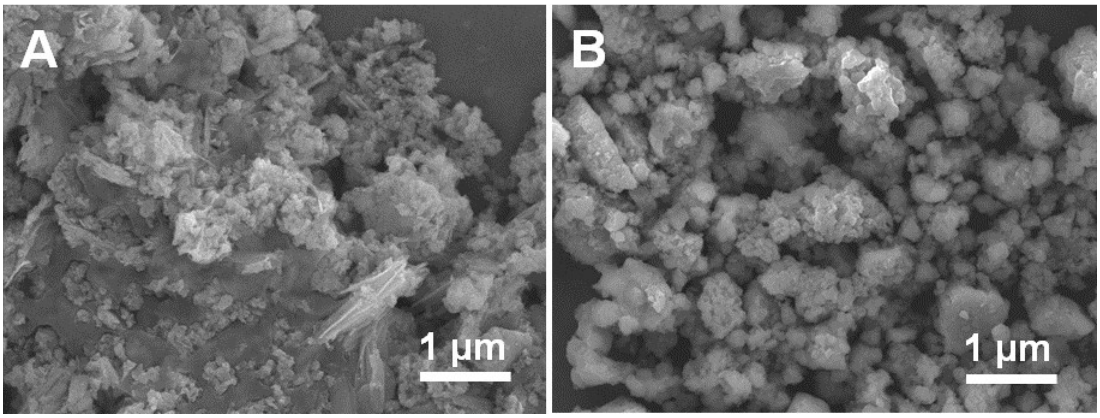

Fig. S4 SEM images of $Fe_2(MoO_4)_3$/C-NS precursor (A) and $Fe_2(MoO_4)_3$-MP precursor (B).

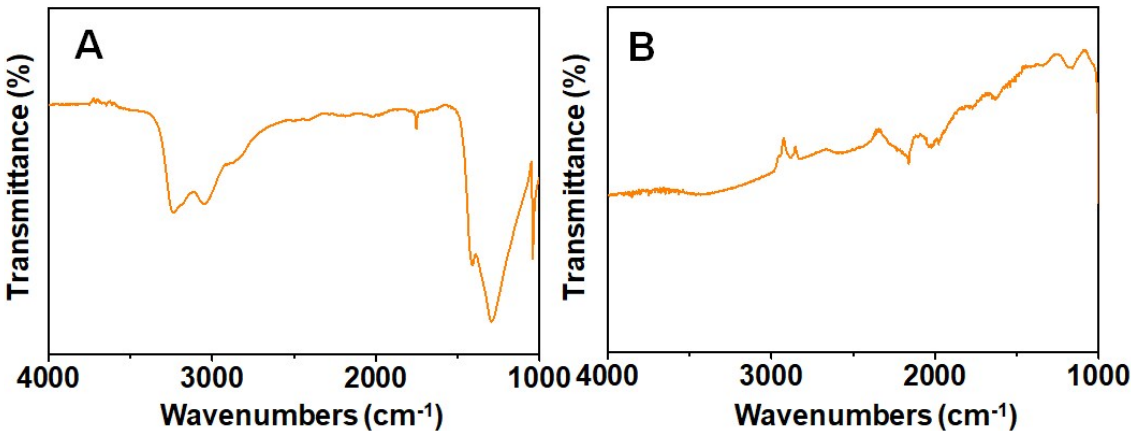

Fig. S5 (A) FT-IR spectroscopy of $Fe_2(MoO_4)_3$/C-NS precursor. (B) FT-IR spectroscopy of $Fe_2(MoO_4)_3$/C-NS sample.

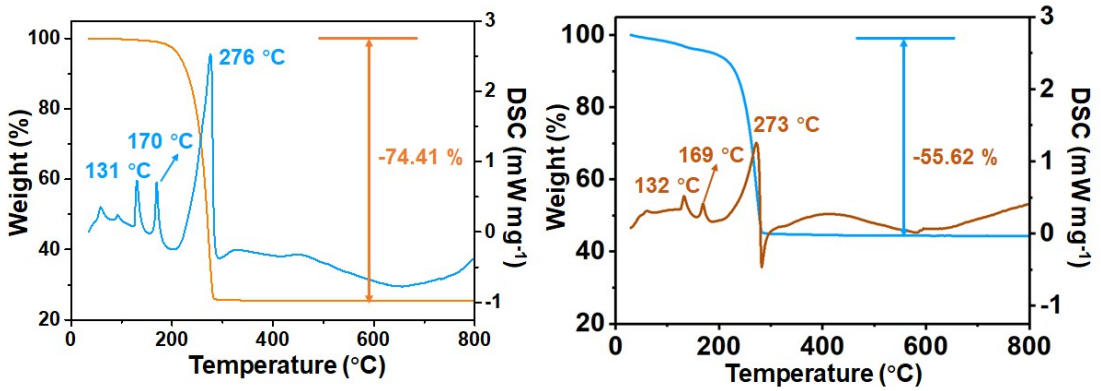

Fig. S6 TG and DSC of $Fe_2(MoO_4)_3$/C-NS precursor (A) and $Fe_2(MoO_4)_3$-MP precursor (B).

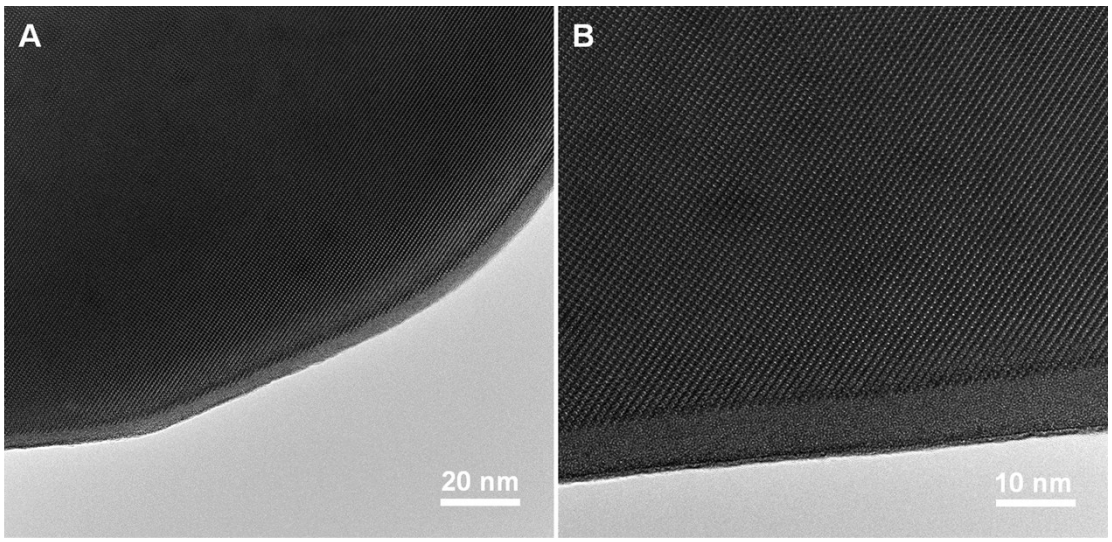

Fig. S7 The HRTEM images of $Fe_2(MoO_4)_3$/C-NS (A, B).

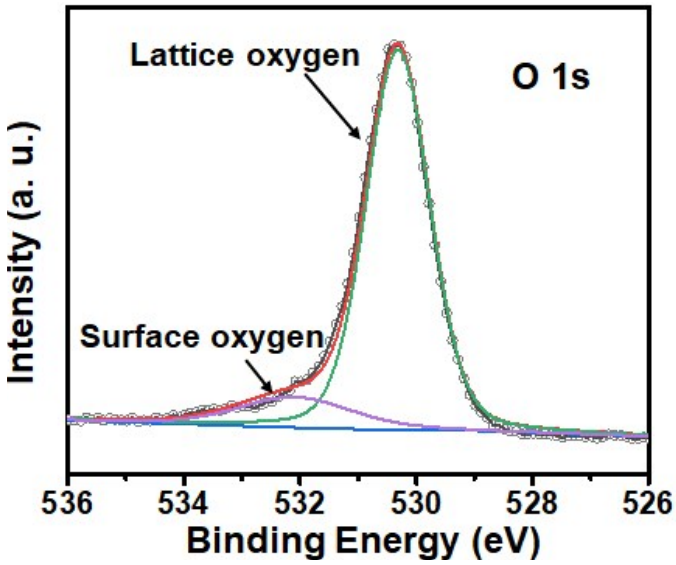

Fig. S8 High-resolution O 1s XPS spectrum of $Fe_2(MoO_4)_3$/C-NS.

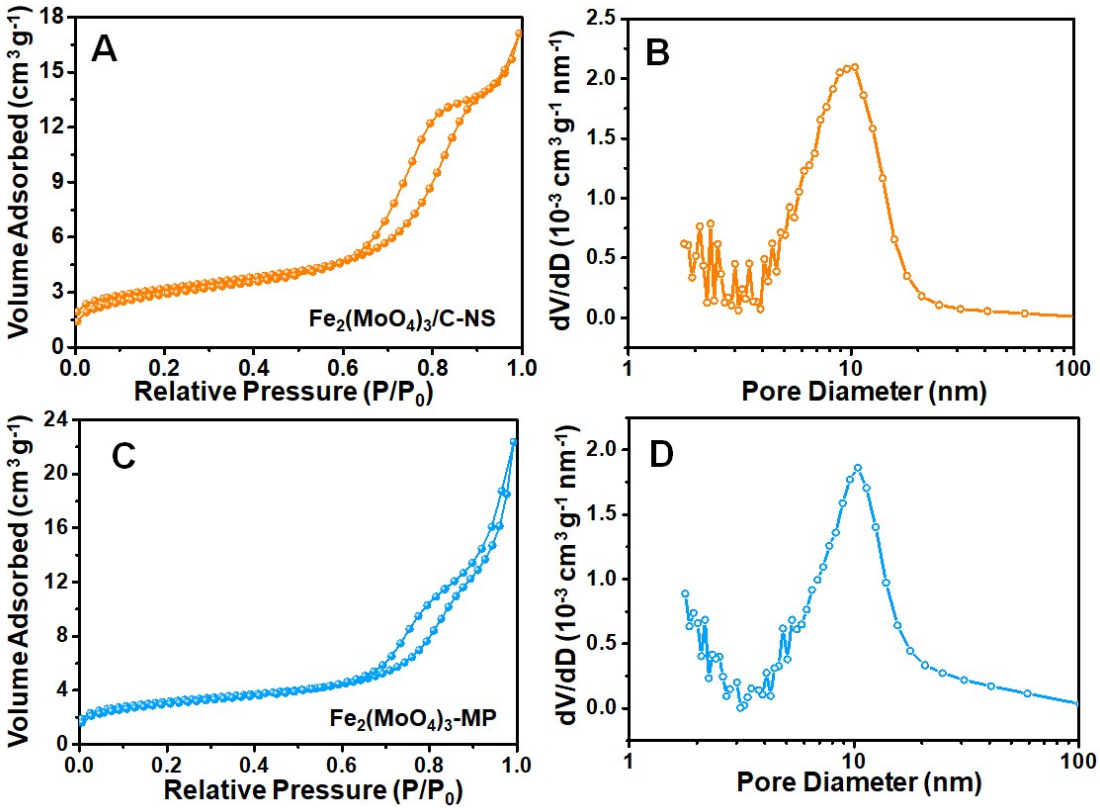

Fig. S9 The N_2 adsorption-desorption isotherms and corresponding BJH pore size distribution curves. (A, B) $Fe_2(MoO_4)_3$/C-NS sample. (C, D) $Fe_2(MoO_4)_3$-MP sample.

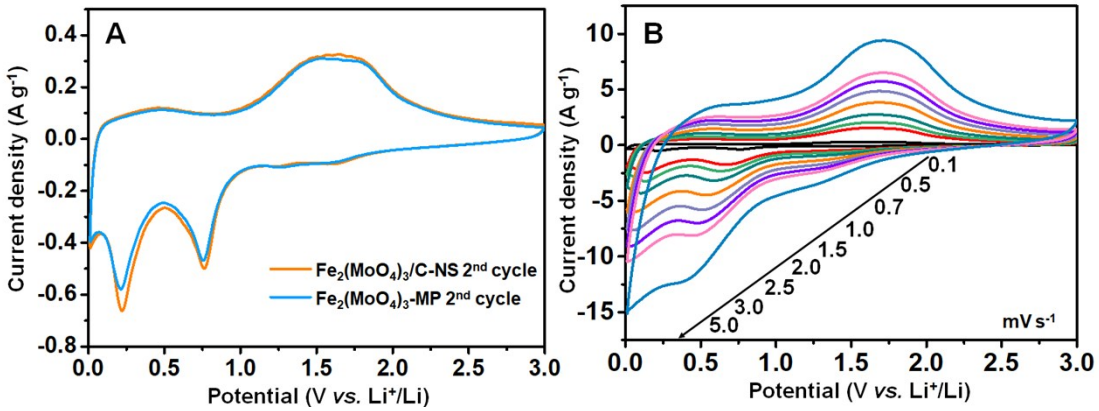

Fig. S10 (A) The second cycle of the cyclic voltammetry curves of $Fe_2(MoO_4)_3$/C-NS and $Fe_2(MoO_4)_3$-MP at 0.1 mV s^{-1} in the potential range from 0.01 to 3.0 V *vs.* Li^+/Li. (B) Cyclic voltammetry curves of $Fe_2(MoO_4)_3$/C-NS at different scan rates from 0.1 to 5 mV s^{-1} in the potential range from 0.01 to 3.0 V *vs.* Li^+/Li.

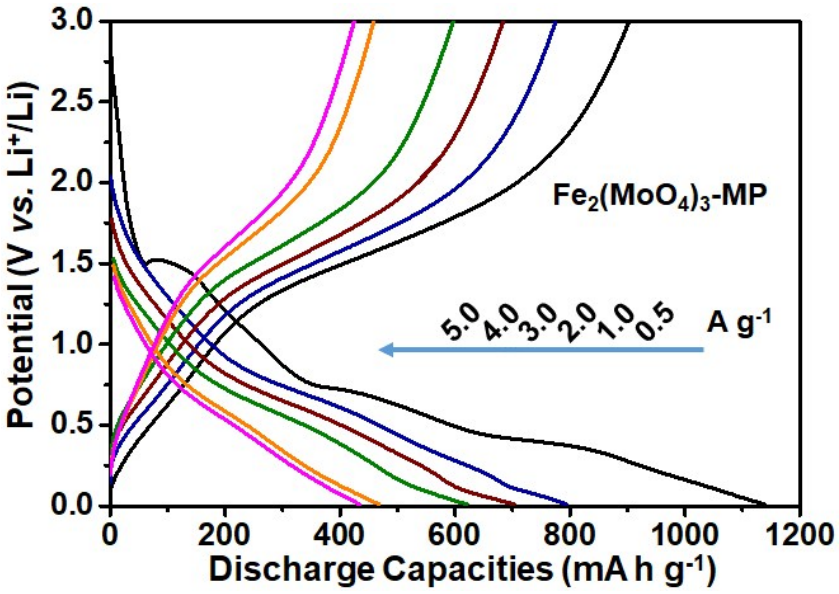

Fig. S11 The discharge-charge voltage profiles of $Fe_2(MoO_4)_3$-MP at different current densities from 0.5 to 5.0 A g^{-1}.

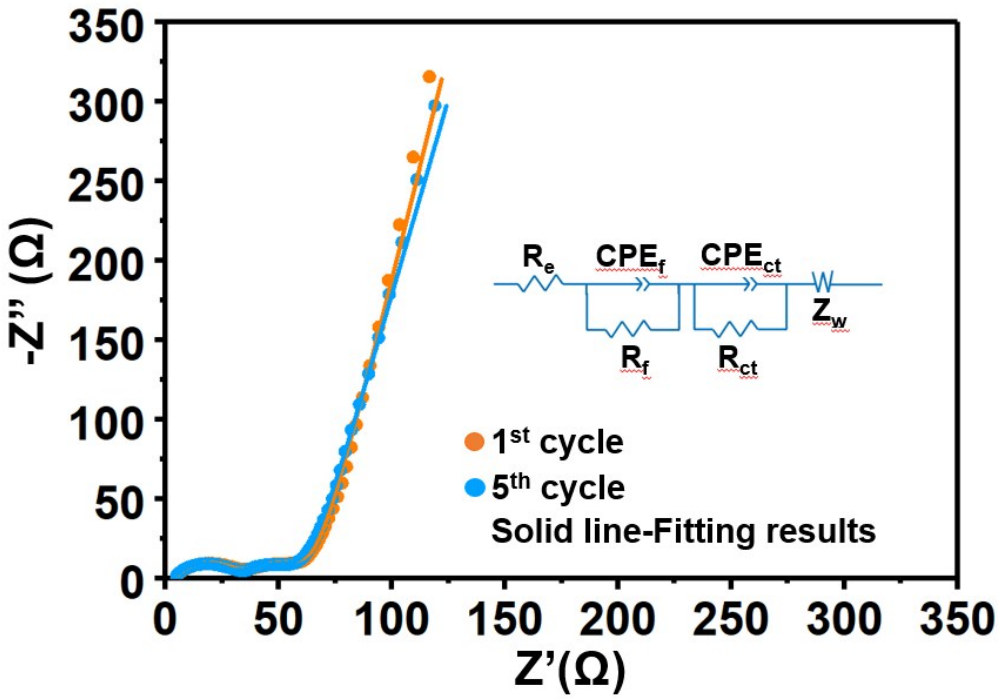

Fig. S12 The typical Nyquist plots of $Fe_2(MoO_4)_3$/C-NS after different cycles.

Table S1 The EIS of $Fe_2(MoO_4)_3$/C-NS electrode at fully charge/discharge states for the first, second, and third cycle.

Discharge/charge	R_f (Ω)	R_{ct} (Ω)
Discharge to 0.01 V (after 1st cycle)	81.5	21.2
Charge to 3.0 V (after 1st cycle)	26.5	65.2
Discharge to 0.01 V (after 2nd cycle)	81.5	38.1
Charge to 3.0 V (after 2nd cycle)	11.0	63.8
Discharge to 0.01 V (after 3rd cycle)	75.3	34.3
Charge to 3.0 V (after 3rd cycle)	12.9	43.8